Food Packaging and Shelf Life 36 (2023) 101058

Contents lists available at ScienceDirect

Food Packaging and Shelf Life

journal homepage: www.elsevier.com/locate/fpsl

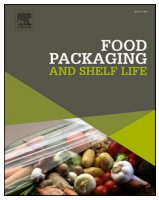

Synthesis and characterization of polyamide 1010 and evaluation of its cast-extruded films for meat preservation

Eva Hernández-García [a], Marta Pacheco-Romeralo [a], Leonor Pascual-Ramírez [b], Maria Vargas [a], Sergio Torres-Giner [a,*]

[a] Research Institute of Food Engineering for Development (IIAD), Universitat Politècnica de València (UPV), 46022 Valencia, Spain
[b] Packaging Technologies Department, AINIA, 46980 Paterna, Spain

ARTICLE INFO

Keywords:
Nylon salts
Bio-based polyamides
Sustainable packaging
Meat preservation
Bioeconomy

ABSTRACT

This study holistically evaluates the potential of polyamide 1010 (PA1010) in the form of monolayer films for meat preservation applications. First, decamethylenediamine and sebacic acid, both derived from natural and renewable castor oil, were used to form a "nylon salt" that was subsequently polymerized at 230 °C by condensation reaction, yielding high-molecular-weight (M_W) PA1010. The resulting fully bio-based polyamide was, thereafter, processed into 145-μm films by cast extrusion and characterized to ascertain their effectiveness in food packaging. Results showed that the PA1010 films were highly transparent, thermally stable up to approximately 340 °C, and very balanced in terms of mechanical strength and ductility, breaking at elongations higher than 150%. The permeability tests revealed that the PA1010 films present a high barrier to water and aroma vapors and a medium barrier to oxygen. Interestingly, the oxygen barrier performance of PA1010 presented low moisture dependence, outperforming currently available biopolymers. Finally, the PA1010 films were applied to package fresh pork fillets in thermosealed bags, proving to be effective in preserving the physicochemical and microbiological quality of meat for up to seven days of storage at 5 °C.

1. Introduction

Food preservation is aimed to extend the shelf life of foodstuffs and provide to consumers safe food products by means of different technologies and materials. Several factors can influence the properties of preserved food, which are determined by the type of foodstuff and, thus, these habitually define the method of preservation (Amit et al., 2017). In recent years, packaging material advances are playing an important role in food preservation (Pardo & Zufía, 2012). Moreover, packaging can perform beyond the conventional protection characteristics since it provides many functions for the contained food product, such as extended preservation, delivery of bioactives, convenience, and communication (Mousavi Khaneghah et al., 2018).

Polymers and additives, that is, plastics, have gained their current relevance in food packaging applications due to they are cost effective, ease to process, and show balanced properties (e.g., flexibility, low density, transparency, etc.) in combination with good versatility (Wohner et al., 2019). This is achieved due to the extensive range of formulations that can be designed specifically to meet product requirements. Indeed, packaging still remains the dominant sectoral use of plastics, representing nearly 40% of the plastic market, in which more than 90% of this corresponds to food preservation applications (Ahmad & Sarbon, 2021). In the area of food packaging, film barrier developments have extensively contributed to reduce food waste due to the quality and safety of food products mostly deteriorate by means of mass transfer phenomena, for example, moisture absorption, undesirable odor absorption, flavor loss, oxygen invasion, and migration into food (Torres-Giner et al., 2019).

Unfortunately, in most cases, single polymers cannot completely meet the barrier requirements for different food packaging uses (e.g., meat products, liquid packaging, dry cereals and snacks, etc.) (Torres-Giner et al., 2019). Therefore, the food packaging industry mainly employs multilayer constructions to fully achieve materials with high-barrier performance and also to support new creative packaging designs and minimize packaging material costs. Multilayer packaging structures consist of up to 12, or even more, symmetric and/or asymmetric layers and/or coatings, adhered using mainly tie resins and designed to be impermeable to gas, aroma, and moisture (Alias et al.,

* Corresponding author.
E-mail address: storresginer@upv.es (S. Torres-Giner).

https://doi.org/10.1016/j.fpsl.2023.101058
Received 6 July 2022; Received in revised form 20 January 2023; Accepted 28 February 2023
Available online 10 March 2023

2022). To this end, the resultant multilayer films must employ different polymers with specific vapor and gas barrier properties to provide a precisely engineered obstacle against a whole range of permeants, such as water vapor, oxygen, carbon dioxide, aroma, or even liquids. However, at the same time, multilayer packaging materials generate severe problems that arise from their disposal, after single use, since they are extremely difficult to separate (Roohi et al., 2018). Indeed, a significant part of municipal solid waste in countries with an advanced economy consists of multilayer structures that cannot be recycled effectively (Kaiser et al., 2018). Therefore, the proper management of post-consumer plastics based on multilayer structures using several petrochemical and non-biodegradable polymers currently represents a fundamental societal challenge and, thus, their replacement with monolayer films can be regarded as a sustainable solution.

Biopolymer-based packaging films are currently in high demand due to the above-described environmental issues and also the scarcity of oil sources (Hernández-García et al., 2021). Biopolymers can be defined as polymers with a "bio-based" origin, polymers that are "biodegradable", or polymers featuring both properties. Bio-based polymers include those produced from renewable resources, both naturally occurring polymers and synthetic polymers produced by using monomers that are obtained from biological sources. Bio-based polymers offer the advantage of using biomass that regenerates (annually) and the unique potential of carbon neutrality. Although bio-based polymers are not necessarily biodegradable, some can offer higher performance than natural polymers and biopolyesters in terms of moisture resistance, processability, thermal stability, ductility, and gas barrier (Torres-Giner et al., 2021). Thus, bio-based polymers can be great candidates to replace fossil derived polymers and meet the current strategies of Circular Economy and Bioeconomy, which promote the use of natural and renewable resources (Philp et al., 2013; Rosenboom et al., 2022).

In this regard, some aliphatic polyamides can be produced partially or totally using natural and renewable monomers (Winnacker & Rieger, 2016). Bio-based polyamides, also called "green nylons", offer high barrier to vapors and gases, resulting in ideal candidates for food preservation applications (Del Nobile et al., 2002). Among bio-based polyamides, polyamide 1010 (PA1010) can be produced from the castor oil derivatives 1,10-decamethylenediamine and sebacic acid. In particular, PA1010 can show comparable properties in terms of flexibility and thermal resistance, or even higher, than those of long-chain polyamide 12 (PA12) derived from petroleum (Quiles-Carrillo et al., 2017). Thus, food packaging articles made in the form of monolayer structures of PA1010 are expected to be very promising since these can show high performance and, thus, they would be easier to recycle and also more aligned with the Circular Economy principles (Češarek et al., 2020).

The present study originally explores and evaluates the development of packaging films of fully bio-based PA1010 to replace petrochemical multilayer films for food preservation applications. To this end, the synthesis of PA1010 was carried out by polycondensation reaction using a nylon salt previously prepared by means of natural and renewable monomers. Then, the newly produced biopolymer was cast-extruded in the form of films and characterized in terms of their optical, thermal, mechanical, and barrier properties. Finally, the food packaging application of the resultant PA1010 films was validated by packaging fresh pork meat fillets and assessing their shelf life for a period of 15 days.

2. Materials and methods

2.1. Materials

Both 1,10-decanediamine or decamethylenediamine, with a CAS number 646–25–3, molecular weight (M_W) of 172.31 g/mol, and purity of 97%, and sebacic acid or decanedioic acid, with CAS number 111–20–6, M_W of 202.25 g/mol, and 99% purity, were purchased at Sigma-Aldrich S.A. (Madrid, Spain). Ethanol absolute (EtOH) and D-limonene were also obtained from Sigma-Aldrich S.A. Magnesium nitrate ($Mg(NO_3)_2$) was supplied by Panreac Química, S.L.U. (Castellar del Vallés, Spain).

Fresh pork meat was purchased in Consum S. Coop. (Valencia, Spain), a local supermarket. The following microbiological media were all provided by Scharlab S.L. (Barcelona, Spain): Buffered peptone water, Violet Red Bile Agar (VRB), and Plate Count Agar (PCA). Man, Rogosa, and Sharpe (MRS) agar was supplied by Labkem-Labbox (Barcelona, Spain).

2.2. Polymerization of PA1010

Synthesis of PA1010 was performed in two steps, that is, preparation of a "nylon salt" and subsequent polymerization of the salt in a glass reactor. In a first step, the monomer salt was prepared based on the procedure described by Chen et al. (2019). Briefly, decamethylenediamine and sebacic acid were first dissolved in EtOH at 40 wt% at room temperature and 10 wt% at 55 °C, respectively, under magnetic stirring. Then, the alcoholic diamine solution was slowly added dropwise to the diacid one for 20 min under continuous stirring, using a diamine-to-diacid molar ratio of 1.05:1.00. The resultant mixture solution was left for 30 min at 55 °C under mild stirring conditions and, thereafter, placed in an ice bath for another 1 h to promote salt precipitation. The supernatant liquid was decanted and the formed salt was washed with EtOH several times until archiving a neutral pH value. The suspension was filtered (Qualitative filter, Prat Dumas, Labkem-Labbox, Barcelona, Spain) and recrystallized with an EtOH/water mixture (10:1 vol/vol). The resultant white salt was dried for 8 h in a vacuum oven (VaciotermT, JP Selecta S.A., Barcelona, Spain) at 60 °C.

In a second step, polymerization of the "nylon salt" was performed in a 1000-ml glass batch reactor with a 5-neck lid. As shown in Fig. 1, the polymerization system consisted of a glass polymerization unit (Fig. 1a)

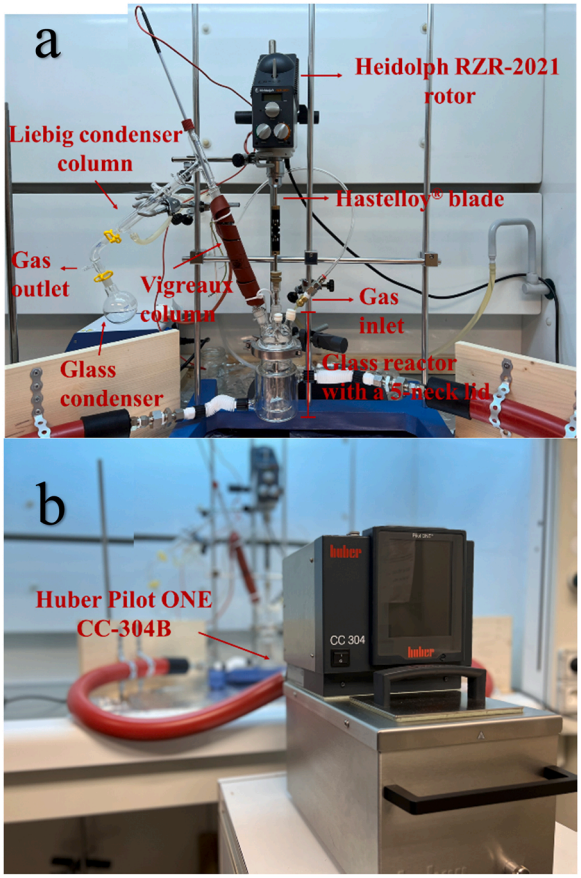

Fig. 1. Polymerization unit (a) connected to the heating station (b).

connected to a heating station (Fig. 1b). On the one hand, the glass reactor was connected to a gas inlet, a stirring system composed of a Heidolph RZR-2021 rotor (Heidolph Instruments GmbH & Co. KG, Schwabach, Germany) equipped with a Hastelloy® blade, and gas outlet with a Vigreaux column. The latter was heated at 135 °C to condensate the diamine vapor and connected to a Liebig condenser column with an open gas exit and graduated round 100-ml glass flask. On the other, the heating station was a Huber Pilot ONE CC-304B (Peter Huber Kältemaschinenbau AG, Offenburg, Germany). This was based on a stainless-steel bath of silicon oil (SilOil P20.275.50, Peter Huber Kältemaschinenbau AG), which allowed for controlling the reactor temperature.

For the polycondensation reaction, approximately 300 g of salt was placed in the reactor. Prior to start polymerization, the reactor unit was purged for 75 min with a constant nitrogen flow-rate of 200 ml/min at room temperature and 25 rpm to remove oxygen and moisture in the reactor headspace. After purging, the gas system was closed with a septum and the system was left under an inert atmosphere and positive pressure. Then, temperature was raised to 230 °C for a time span of 60 min, whereas the reaction media was vigorously stirred at 100 rpm. After this, once the mixture was homogenized, the nitrogen inlet was opened (50 ml/min) and the reaction was kept at 230 °C for 3 h under stirring at 75 rpm (2 h) and 50 rpm (1 h). Finally, the reactor system was allowed to cool, under inert atmosphere, to room temperature. The resultant white solid mass was removed from the reactor and milled in a IKA M20 basic analytical mill (IKA®-Werke GmbH & Co. KG, Staufen, Germany). The powder was stirred for 4 h with deionized water at 55 °C and was left overnight at room temperature. After this, the mixture was filtered, gently washed with EtOH, and dried at 60 °C for 8 h in a vacuum oven (VaciotermT). Different batches were prepared to obtain approximately 1 kg of biopolymer powder, which was stored in aluminum trays inside a desiccator for at least one week to eliminate the remaining humidity.

2.3. Viscosity of PA1010

The viscosity number (VN) of PA1010 was determined following the ISO 307:2007 standard (ISO, 2007) by dissolving the dried powder sample in sulfuric acid (96%, Vidrafroc S.A., Barcelona, Spain) at 25 °C and measuring the viscosity number with a Type II Ubbelohde viscometer (Vidrafroc S.A.). The VN value, expressed in cm^3/g, was calculated using Eq. 1:

$$VN = \left[\left(\frac{\eta}{\eta_0}\right) - 1\right] \times \frac{1}{C} \quad (1)$$

Where η ($N/m^2 \cdot s$) corresponds to the viscosity of the polymer solution in the specified acid, η_0 ($N/m^2 \cdot s$) is the viscosity of the solvent, η/η_0 is the relative viscosity of the polymer solution, and C (0.005 g/cm^3) is the concentration of the polymer solution.

Then, the value of M_W (g/mol) was estimated from the Mark–Houwink–Sakurada expression, shown in Eq. 2:

$$\eta = K \times M_W{}^{\alpha} \quad (2)$$

Where η (cm^3/g) is the intrinsic viscosity, also known as Staudinger index, whereas K and α are the coefficient and molecular parameters, which describes the hydrodynamic interaction between the solvent and the macromolecules. The M_W value of PA1010 was estimated using the previous experimental data reported for polyamide 6 (PA6) (Li et al., 2003) and PA12 (Wudy & Drummer, 2019).

2.4. Thermal analysis of PA1010

2.4.1. Thermogravimetric analysis

Thermal stability was evaluated by thermogravimetric analysis (TGA) in a TGA 1 STARe System analyzer from Mettler-Toledo, Inc. (Greifensee, Switzerland). In the case of the "nylon salt", to ascertain the thermal stability of the raw material during polymerization, the procedure consisted of a heating ramp from 25 °C to 230 °C at 3.3 °C/min, followed by an isotherm at 230 °C for 3 h. For PA1010, the heating program was set from 25 °C to 600 °C at a heating rate of 20 °C/min, using powder. Samples were analyzed with a constant flow-rate of nitrogen of 10 ml/min to achieve an inert atmosphere, whereas approximately 3 mg of sample was used for the measurements. The thermogravimetric and derivative curves were analyzed using a STARe Evaluation Software (Mettler-Toledo, Inc.) to obtain the temperature at 5% weight loss ($T_{5\%}$), the so-called onset degradation temperature, and the degradation temperature (T_{deg}) derived from the peak value of the first derivative.

2.4.2. Differential scanning calorimetry

Differential scanning calorimetry (DSC) was carried out to obtain thermal transitions using a DSC 1 STARe System model from Mettler-Toledo, Inc. Around 5 mg of salt or film sample was placed in hermetic aluminum sealed pans of 40 μl that were calibrated previously by means of indium standard. Dry reducing atmosphere was used to perform the analysis, using nitrogen flowing at 40 ml/min. Both the salt and resultant PA1010 powder were subjected to a three-step program at 10 °C/min. The first heating scan was applied from − 40 °C to 260 °C, then followed by a cooling scan to − 40 °C, and a final second heating to 260 °C. From the cooling scan, the normalized enthalpy of crystallization (ΔH_C) and crystallization temperature from the melt (T_C) were obtained, whereas the glass transition temperature (T_g), normalized cold crystallization enthalpy (ΔH_{CC}), cold crystallization temperature (T_{CC}), normalized enthalpy of melting (ΔH_m), and melting temperature (T_m) were obtained from the second heating scan. The percentage of crystallinity (X_C) of PA1010 was determined using Eq. 3:

$$X_C = \left[\left(\frac{\Delta H_m - \Delta H_{CC}}{\Delta H_m 0}\right)\right] \times 100 \quad (3)$$

Where ΔH_m^0 (J/g) represents the theoretical melt enthalpy of a fully crystalline PA1010, with a value of 244 J/g (Yan & Yang, 2012).

2.5. Extrusion of PA1010

The dried PA1010 powder obtained from the polymerization process was, thereafter, cast-extruded into films using a laboratory-scale cast-roll machine. This is based on a single-screw extruder TEACH-LINE® E 20 T with a screw diameter of 20 mm and length of 25 x D, having a flat die of 120 mm in width, connected to a flat-film take-off unit Chill-Roll TEACH-LINE® CR 72 T, both from Dr Collin GmbH (Ebersberg, Germany). Fig. 2 shows the cast-roll machine employed for the extrusion process (Fig. 2a) and the calender flat-film system used to obtain the films (Fig. 2b). The latter was designed as a three-roll unit with an upper adjustable smoothing roll, a central fixed roll, and a lower cooling roll. The temperature profile was set as 35 °C (feeding)–210–210

Fig. 2. Cast-roll machine used for the production of flat films (a) with detail of the calender flat-film system (b).

210–210–230 °C (head) using a speed of 30 rpm. By adjusting the speed of the calendar and the drag, PA1010 films with an average thickness of approximately 145 μm were produced.

2.6. Film characterization

2.6.1. Film thickness and conditioning

The film thicknesses were measured at sixteen random points using a digital electronic micrometer (Palmer model COMECTA, Barcelona) having an accuracy of 0.001 mm as described in previous study (Hernández-García et al., 2022a). The film samples were conditioned in desiccators containing saturated solutions of $Mg(NO_3)_2$ at the conditions of 25 °C and 53% relative humidity (RH).

2.6.2. Optical evaluation

The optical properties were determined using a MINOLTA spectrocolorimeter (model CM-5, Minolta Co., Tokyo, Japan) by measuring, from 400 to 700 nm, the reflection spectrum of the film samples. The transparency was measured by means of the internal transmittance (T_i), applying the Kubelka-Munk theory (Hutchings, 1999). The illuminant D65 and observer 10° was used to determine, in triplicate, the CIE L*a*b* (CIELAB) color coordinates as well as the chroma and hue chromatic parameters.

2.6.3. Tensile tests

The Stable Micro System TA-XT plus Universal Testing Machine (Haslemere, England) was employed to analyze the mechanical behavior of the films according to the guidelines of ASTM standard method D882 (ASTM, 2001). The samples, sizing 25 mm × 100 mm, were mounted in the film's extension grip and then stretched until breaking at a rate of 50 mm/min. Force-deformation curves were attained and transformed into stress-strain curves by considering sample dimensions and degree of deformation. Mechanical tests were carried out in a room at the controlled conditions of 25 °C and 60% RH.

2.6.4. Permeability measurements

The modification of the ASTM E96–95 gravimetric method (ASTM, 1995) was followed to determine gravimetrically, using Payne permeability cups, the water vapor permeability (WVP). This test was carried out at 25 °C and a RH gradient from 53% to 100% since it represents conditions of intermediate humidity. The analytical balance ME36S with an accuracy of ± 0.00001 g from Sartorius (Fisher Scientific, Hampton, NH, USA) was used to weigh periodically for 24 h the cups at intervals of 1.5 h once the steady state was reached. The water vapor permeance was determined from the water vapor transmission rate (WVTR), which was obtained from the slope of the weight loss vs. time, and then corrected for permeant partial pressure. Permeance was thereafter corrected with film thickness to obtain WVP. A similar procedure was followed to determine limonene permeability (LP), where 5 ml of $_D$-limonene was placed instead of water inside the Payne permeability cups under the same controlled room conditions of 25 °C and 53% RH. In both cases, cups with aluminum films were used as control samples to estimate and subtract the vapor loss through the sealing. Also films without water and $_D$-limonene were used to correct the mass corresponding to the vapor uptaken in the film samples during analysis. All the vapor permeability measurements were performed in triplicate.

The ASTM Standard Method D3985–05 (ASTM, 2010) was applied to attain oxygen permeability (OP). Three film replicates of each formulation of 50 cm^2 were measured using an Oxygen Permeation Analyser (Model 8101e, Systech Illinois, Thame, UK) at 25 °C and varying RH from 0% to 90%. The oxygen permeance was obtained from the oxygen transmission rate (OTR), which was corrected with the gas partial pressure between the two sides of the film. Then, permeance was corrected with film thickness to obtain OP. Measurements were also recorded in triplicate.

2.7. Evaluation of pork meat shelf life

2.7.1. Pork meat sample preparation

All work surfaces and utensils were initially cleaned and disinfected with 96% ethanol to avoid cross contamination. Then, the PA1010 films were exposed for 30 min to UV light for sterilization in a laminar flow cabinet (Bio II Advance, Telstar, Fisher Scientific S.L., Madrid, Spain). After this, using a slicer, pork meat was cut into 10 g-fillets and immediately thermosealed to form bags in sterilized film samples (area 10 cm × 10 cm) using a SAECO Vacio Press Elite vacuum packing machine (Barcelona, Spain). Themosealing was perfomed by the application of 3 cycles of 6 s each at a temperature of 80 °C. All packaged samples were stored for up to 15 days under refrigerated conditions (5 °C).

2.7.2. Physicochemical characterization

Changes in weight loss, pH, lipid oxidation, and color were analyzed in the packaged pork meat during storage. The weight loss was quantified as a function of storage time using the ME36S Sartorius analytical balance. The pH was determined by direct insertion into the pork meat of the electrode probe using a digital pH meter from Mettler-Toledo, Inc. Three fresh pork meat samples were used for characterization of the raw material (pork meat control) at 0 day and two film samples were analyzed at 3, 7, 11, and 15 days. Ten repetitions were performed taken five measurements for each sample.

Lipid oxidation was determined as described by Siu and Draper (1978). Pork meat samples were analyzed at the beginning (0 day) and after 15 days. The experiment was performed in triplicate and expressed as mg of malondialdehyde (MDA)/kg of sample.

Using the D65 illuminant and 10° observer, the color (CIE L* a* b* color coordinates) of the packaged meat in the PA1010 film was measured from 400 to 700 nm with the MINOLTA spectrocolorimeter model CM-5 on the sample surface at six random point. Three film samples were analyzed at the following days: 0, 3, 7, 11, and 15. Six measurements were taken for each sample.

2.7.3. Microbiological analysis

Packaged pork meat was tested for their microbial growth at 0, 3, 7, 11, and 15 days (Hernández-García et al., 2022b). Using sterile forceps and scalpels, a total of 10 g of meat sample was aseptically taken, then placed into sterile stomacher filter bag with 90 ml of peptone water (Scharlab S.A.), and homogenized for 3 min using a Masticator paddle blender from IUL Instruments (Barcelona, Spain). Then, serial dilutions were plated and covered with selective media: VRB for total coliforms, PCA for total aerobic counts (TAC), and MRS for lactic acid bacteria (LAB). TAC and total coliforms were incubated at 37 °C for 48 h, while LAB were incubated for 72 h at 30 °C. Bacterial colonies were counted after incubation. Microbial counts were tested in duplicate for the packaged and control sample at each time. The bacterial counts were expressed as $\log_{10}$ colony-forming units per gram of sample (log CFU/g).

2.8. Statistical analysis

The Statgraphics Centurion XVI software from Manugistics Corp. (Rockville, Md.) was used to subject the pork meat properties evaluated during storage to an analysis of variance (ANOVA). Fisher's least significant difference (LSD) procedure at the 95% confidence level was used.

3. Results and discussion

3.1. PA1010 synthesis and thermal properties of nylon salt

Polyamides are linear and semicrystalline condensation polymers with recurring amide groups as the integral part of the main polymer chain. Its "nylon salt" was first produced, as the starting material to

prepare high-M_W bio-based PA1010. This was carried out by precipitation in ethanol solutions using stechiometric molar quantities of decamethylenediamine and sebacic acid, but with a slight excess of diame to consider potential monomer losses during the "nylon salt" preparation. Subsequently, having a careful control of the temperature during the reaction, the salt was polymerized in the reactor.

Prior to perform the polymerization reaction, the thermal stability and characteristics of the salt was ascertained by TGA and DSC and Fig. 3 gathers the resultant thermal curves. Fig. 3a shows the TGA curve, where the thermal conditions faced during polymerization were simulated. This was based on a heating ramp from 25 °C to 230 °C at 3.3 °C/min, followed by an isotherm for 3 h at 230 °C, all under nitrogen atmosphere. At these conditions, the setpoint temperature of 230 °C was reached after approximately 62 min. During heating, it was observed that the salt presented a mass loss of ~1% at 100 °C, which can be ascribed to the evaporation of the remaining solvents or sorbed water. This phenomenon was followed by a more intense mass loss, which was seen as a sharp peak starting at nearly 176 °C and centered at ~189 °C. This mass loss can be associated to the release of water during formation of the amide bonds by polycondensation, with a value of nearly 12%. Thereafter, during the isothermal conditions at 230 °C, the sample progressively lost mass at a lower rate, up to reaching a plateau after approximately 200 min. In particular, the mass loss associated to this stage was only 4%, which can be related to the progressive water released during the growth of the biopolyamide chains, suggesting the absence of thermal degradation.

The thermal transitions of the salt were further studied by means of DSC. Fig. 3b confirmed the melting and subsequent polymerization of the salt to form PA1010, as also observed during TGA. One can notice that it melted at approximately ~180 °C, yielding a second melting peak at ~199 °C. The latter can be related to the melting of the oligomer or prepolymer formed from the salt during heating in the DSC pans. During cooling, the prepolymer also crystallized, resulting in a T_C value of ~177 °C, and then melted during second heating, with a value of T_m of ~197 °C. Similar second-order thermal transitions have been previously reported for PA1010 (Quiles-Carrillo et al., 2017), confirming the formation of the oligomer or low-M_W biopolyamide.

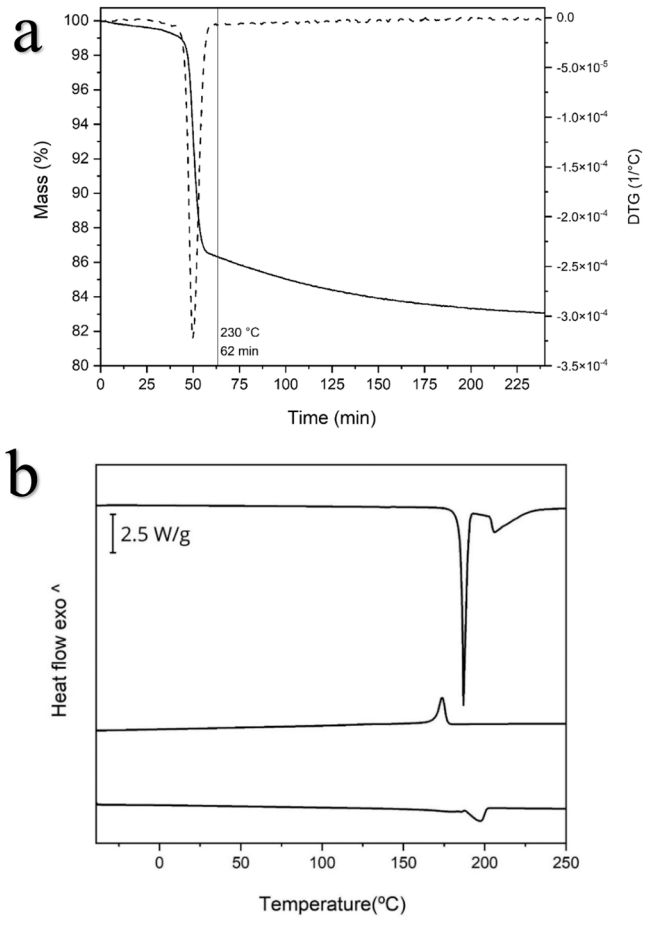

Fig. 3. (a) Thermogravimetric analysis (TGA) curves; (b) Differential scanning calorimetry (DSC) curves corresponding to, from top to bottom, first heating, cooling, and second heating of the "nylon salt".

Finally, the viscosity number of the synthesized PA1010 in the above-described conditions was determined, yielding a value of 130 ± 5 cm^3/g. According to the Mark–Houwink parameters reported for PA6 (Li et al., 2003) and PA12 (Wudy & Drummer, 2019), this value of viscosity corresponds to a M_W in the range of 0.41–1.30 × 10^5 g/mol. Several biopolyamides have showed M_W values from ~2500 g/mol upward, depending on the synthesis conditions and the proposed applications (Winnacker & Rieger, 2016). Similarly, Li et al. (2003) reported viscosity values ranging from 84 to 126 cm^3/g for polyamide 1214 (PA1214). Values varied as a function the reaction conditions, including temperature, pressure, and time. Furthermore, Cui et al. (2004) showed M_Ws varying from 7200 g/mol to above 1.30 × 10^4 for even–odd nylons based on undecanedioic acid, ascribing the low values attained to the high volatility of the various amines used to prepare the polyamides. Therefore, this value of M_W is relatively high and, thus, it is expected to be adequate for melt-mixing processes. Furthermore, the viscosity value was close to those of commercial PA1010 produced in large reactors for injection molding and extrusion processes, that is, 160 and 220 cm^3/g, respectively (Quiles-Carrillo et al., 2020). The relatively high viscosity attained in the laboratory sample can be due to the fact that PA1010 was produced from the two-step procedure, first forming-salt and then melting-polycondensation, which was prepared using a controlled dicarboxylic acid/diamine ratio at room temperature and could avoid premature chain termination.

3.2. Thermal properties of PA1010

The PA1010 powder was also subjected to thermal analysis to ascertain both stability and thermal transitions of the newly produced biopolymer. Fig. 4 provides the TGA curves (Fig. 4a) and DSC thermograms (Fig. 4b) of the biopolymer. As can be seen, PA1010 was stable up to nearly 340 °C, showing a T_{deg} of 468.3 ± 2.4 °C. Similar values have been attained for PA1010 (Quiles-Carrillo et al., 2017), describing that a β-C-H transfer reaction mechanism that produces ketoamides, as the primary decomposition products, is involved in thermal degradation. This confirms the high thermal stability of PA1010, which can be successfully applied in most food packaging applications and also in nearly unlimited industrial processing conditions of plastics.

In terms of thermal transitions, the biopolyamide showed a second order one that is related to its T_g, in the 40–60 °C range, which is difficult to elucidate by DSC due to its reduced amorphous phase (Quiles-Carrillo et al., 2017). Nevertheless, the T_g value of PA1010 has been analyzed thermomecanically, showing a value of approximately 50 °C (Quiles-Carrillo et al., 2020). As can be observed in the thermographs, the biopolymer crystallized from the melt during cooling, showing a single T_C value of 170.1 ± 0.7 °C. One can further observe that PA1010 displayed a single melting peak during both heating scans, with a T_m value of 200.6 ± 0.8 °C. This result suggests the presence in the biopolymer of a single crystalline form. However, a shoulder was also observed at lower temperatures, which can be related to the melting process of less perfect crystallites of PA1010 that could recrystallize and thereafter melt at higher temperature (Yan & Yang, 2012). This thermal behavior differs from that of short-chain polyamides, such as PA6 and polyamide 66 (PA66), and also other even–even polyamides, which tend to exhibit a polymorphism behavior and display multiple melting behaviors during heating (Logakis et al., 2009). These thermal properties place PA1010 in between short-chain PA6 (~221 °C) (Cho & Paul,

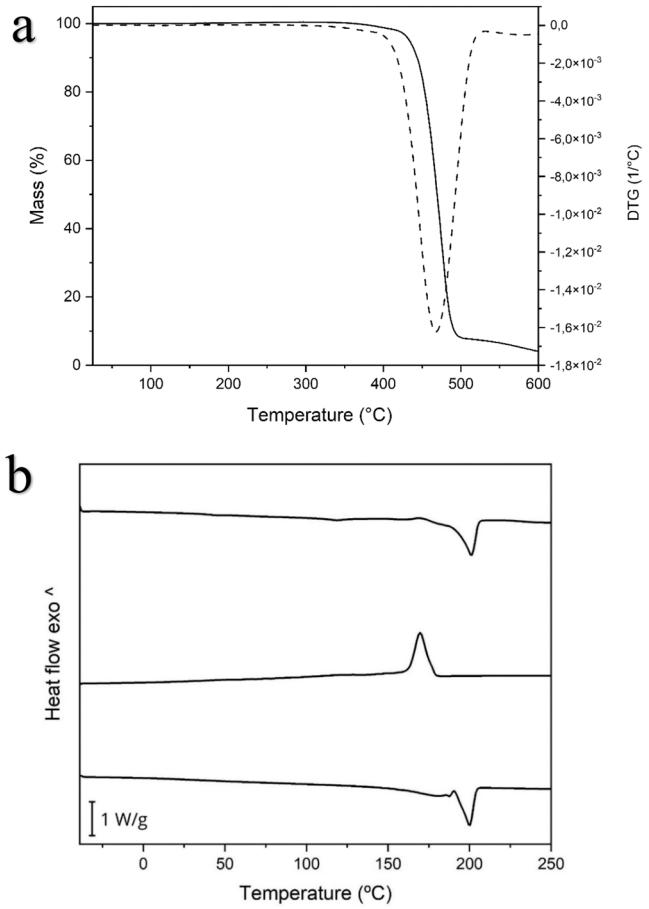

Fig. 4. (a) Thermogravimetric analysis (TGA) curves; (b) Differential scanning calorimetry (DSC) curves corresponding to, from top to bottom: first heating, cooling, and second heating of polyamide 1010 (PA1010).

2001) and medium- or long-chain PA12 (~179 °C) (Yan et al., 2011). The thermal profile of PA1010 is optimal from a point of view of being processable by melting routes at moderate temperature, but also still stable for heating treatments below 200 °C (e.g., microwave). Furthermore, in terms of the amount of crystallinity, the sample yielded a value of 49.7%. This was obtained from the melting enthalpy during the second heating, after removing thermal history. This value of crystallinity is higher than that found in other bio-based polyamides, such as polyamide 610 (PA610) and polyamide 1012 (PA1012), which mainly derives from the symmetrical chain structure of PA1010 since the C10 chemical structure is shared by both the diamine and dicarboxylic acid (Quiles-Carrillo et al., 2017). Indeed, chain-folded sheets are formed from even-even polyamides, where linear hydrogen bonding to one another participate in the amide groups. This favors the achievement of a regular spacing along the polyamide chains of the amide groups, resulting in a polyamide with a relatively high crystallinity and, hence, high mechanical and barrier performance.

3.3. Optical evaluation of PA1010 films

The resultant PA1010 powder was melt-processed by cast extrusion to yield 145-μm films and their properties were analyzed to ascertain their value in food packaging applications. Fig. 5 represents the spectral distribution curve of the percentage of T_i of the PA1010 film as a function of wavelength (λ).

The film sample showed, as can be seen in the graph, high T_i values, in the 83–87% range. This result indicates that PA1010 yielded transparent films since the sample highly transmitted light. In terms of optical

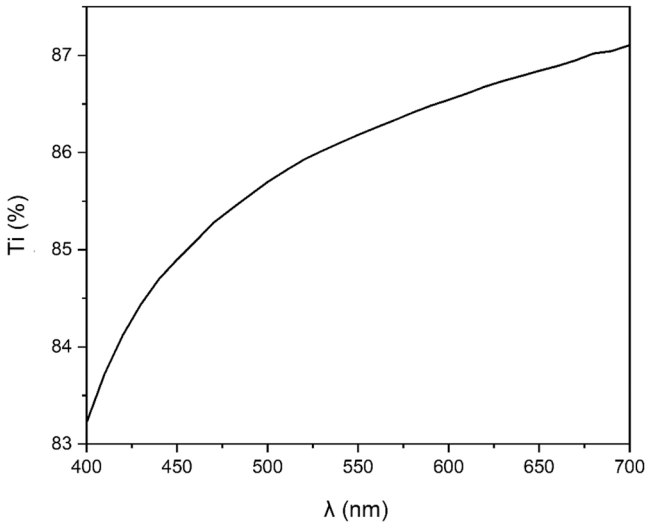

Fig. 5. Spectral distribution curve of the percentage of internal transmittance (T_i) of polyamide 1010 (PA1010) films.

properties, the film sample showed high brightness, measured as L*, with a value of 88.0 ± 0.63. In relation to the a* and b* color coordinates, values of − 1.2 ± 0.04 (slightly green) and 3.1 ± 0.09 (pale yellow) were respectively obtained. This resulted in a film sample with a hue or tone (h_{ab}*) of 11.8 ± 1.89, having a color saturation or chroma (C_{ab}*) of 3.4 ± 0.09, which are related to a greenish yellow or lime color of low intensity. Moreover, the values of T and O, corresponding to the transparency and opacity, were 0.400 ± 0.026 and 0.010 ± 0.001, respectively, confirming the development of highly transparent films. This low color intensity and transparency is similar to that found in polylactide (PLA) films but highly differs from biodegradable polyhydroxyalkanoates (PHAs), which tend to form opaque films with a yellow hue and low transparency (Arrieta et al., 2014; Hernández-García et al., 2023). Therefore, PA1010 can be of interest when the "see-through" capability is needed, for example, in films for lids or stand-up pouches in food packaging applications (Cozzolino et al., 2014).

3.4. Mechanical properties of PA1010 films

The mechanical properties of the PA1010 films were also evaluated

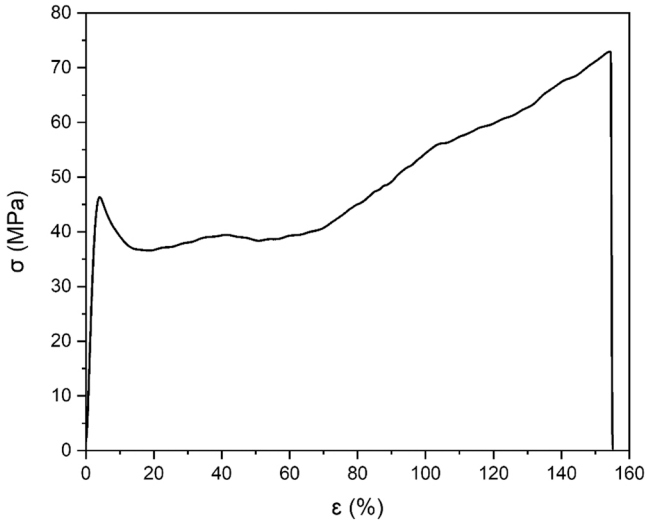

Fig. 6. Typical tensile stress-strain curve of polyamide 1010 (PA1010) films.

to ascertain their performance for food packaging applications. Fig. 6 shows the typical tensile stress-strain curve of the PA1010 films at room temperature. The sample showed a tensile modulus (E) and strength at yield (σ_y) of 762.1 ± 57.5 MPa and 45.4 ± 3.3 MPa, respectively, which can be ascribed to a material with an intermediate elasticity and high resistance. Finally, the film showed a value of elongation at break (ε_b) of 155.06 ± 36.3%, indicating that the PA1010 film was relatively ductile and can be thus suitable for flexible packaging applications. The mechanical performance of the PA1010 film offers a remarkable advantage in comparison with most of the biodegradable polyesters being currently researched for food packaging applications. For instance, PLA and PHA articles are characterized by showing high fragiliy, with ε_b values below 5%, so it makes necessary the development of blend formulations with highly ductile biopolymers (Quiles-Carrillo et al., 2018).

It can also be observed that the PA1010 film sample exhibited double yielding during deformation, reaching a value of maximum tensile strength (σ_{max}) of 71.2 ± 5.8 MPa. This second-yielding phenomenon seems to originate from a recrystallization process, thus increasing the crystallinity and hardening of PA1010 in the force orientation. The so-called "strain hardening" has reported to increase the crystallinity of polyamides when compared with their unstretched samples (Shan et al., 2005). Although this second-yielding phenomenon has not been fully elucidated, it has been explained by the local melting-recrystallization theory, which supports that stress concentration causes less perfect crystallites to partially melt and recrystallize (Gupta & Rana, 1998). Other researchers suggested that multiple yielding is related to the coupling of the amorphous region with the crystalline one and, therefore, both inter- and intra-links should be considered (Shan et al., 2007). In the particular case of PA1010, crystal orientation by tensile force was studied (Cui & Yan, 2005), indicating that the crystallization rate can be accelerated with the draw ratio. During stretching, the restriction of hydrogen bonding on methylene segments is reduced by the weakening of hydrogen bonding, which facilitates molecular chain movement and stimulates stretch-induced crystallization. In addition, the partial fracture of hydrogen bonds between the carbonyl (C═O) group and the amino (N–H) group of the adjacent polyamide chain is caused by stretching, resulting in a small amount of free amino groups. In any case, this opens up the possibility to both mono- and biaxially orient PA1010 films, further increasing their mechanical performance, as similar to other polyamides (Rhee & White, 2002).

3.5. Barrier properties of PA1010 films

The barrier performance to vapors and gases of the PA1010 films was analyzed, which is of high application interest for food packaging. Thus, Table 1 shows the values of permeability referred to the water and limonene vapors and also oxygen gas, being all measured at 53% RH. The table also includes the barrier properties of other polyamides and biopolymers of application interest in the field of food packaging for comparison purposes. In relation to WVP, it is worth to note that condensation polymers tend to absorb moisture and, for polyamides, this is highly dependent on their methylene-to-amide (CH_2/CONH) ratio (Del Nobile et al., 2002). Thus, water barrier becomes lower in polyamides with higher amide densities per unit length of chain, whereas polyamides with long-alkane-segments exhibit lower water permeability. In the case of PA1010, the CH_2/CONH ratio is 9 (Quiles-Carrillo et al., 2017), yielding a WPV value of 1.56×10^{-15} Kg·m/m^2·Pa·s. This water barrier performance is one order of magnitude higher than that of PA6, which shows a WVP value of 2.06×10^{-14} Kg·m/m^2·Pa·s at 90% HR (Lagarón, 2011). The WVP value attained was similar but also slightly lower than that of PA12, that is, 3.46×10^{-15} Kg·m/m^2·Pa·s at 85% HR (McKeen, 2017). This permeability difference can be mainly ascribed to the different humidity conditions used for the permeability tests, that is, 53% and 85% RH, since PA12 is expected to have a higher barrier to water due to its higher CH_2/CONH ratio. Furthermore, in comparison with poly(butylene adipate-*co*-terephthalate) (PBAT), PLA, and also poly(3-hydroxybutyrate-*co*-3-hydroxyvalerate) (PHBV), which are biopolymers commonly researched in food packaging, PA1010 outperformed them in all cases. In particular, the permeability to water vapor was in the same range but slightly lower than PHBV, and one order of magnitude lower than PLA and PBAT (Quiles-Carrillo et al., 2019). One can further observe that the permeability to limonene, used habitually as standard to ascertain the barrier to aroma, was also significantly lower than those observed for other biopolymers, showing a value of LP of 1.78×10^{-15} Kg·m/m^2·Pa·s. This certainly confirms the high potential of PA1010 as monolayer material with moisture and aroma resistance for sustainable packaging applications.

Regarding oxygen performance barrier, the PA1010 film yielded a value of 6.59×10^{-19} m^3·m/m^2·Pa·s at 53% RH. This permeability value is very similar to that reported recently by Sun et al. (2019) at 50% RH, that is, 5.02×10^{-19} m^3·m/m^2·Pa·s. This result points out that the permeability to oxygen of PA1010 corresponds to a medium-barrier polymer, as expected due to its intermediate CH_2/CONH ratio. Thus, PA1010 presents an oxygen barrier in between those of short-chain PA6, showing values in the 0.5–2.5 $\times 10^{-19}$ m^3·m/m^2·Pa·s range (Lagarón, 2011), and long-chain PA12, in the 2.0–2.2 $\times 10^{-18}$ m^3·m/m^2·Pa·s range (McKeen, 2017), depending on the % RH. In comparison to the previously mentioned biopolyesters, the oxygen permeability of PA1010 is similar but slightly higher than medium-barrier PHBV, and lower than PLA and, more notably, PBAT (Quiles-Carrillo et al., 2019).

As a condensation polymer, PA1010 shows dependence of oxygen permeability on moisture conditions. Fig. 7 illustrates the OP values of PA1010 as function of %RH. To the best of our knowledge, this is the first analysis reported for a bio-based polyamide and it can be particularly relevant when it is considered to be applied in the form of monolayers that are not protected by external layers of high-water-barrier polymers and then potentially exposed to extreme humidity conditions. Interestingly, the graph revealed a relatively low effect of moisture on permeability to oxygen, which can be ascribed to the fact that the effect of moisture on the oxygen barrier is lower in polyamides with lower content of amide groups and longer carbon chain lengths. One can also further observe that the PA1010 film presented the highest barrier to oxygen at intermediate humidity, that is, 53% RH. Thus, the PA1010 film yielded OP higher values at low %RH, of 8.83 and 7.84 $\times 10^{-19}$ m^3·m/m^2·Pa·s for 0% and 22.5%, respectively. At higher humidity conditions the oxygen barrier was also slightly higher, showing OP values of 7.51 and 7.50 $\times 10^{-19}$ m^3·m/m^2·Pa·s for 75% and 90% RH, respectively. This performance reduction at extreme humidity conditions is ascribed to a misbalance established by the sorbed water molecules that participate in the polyamide interchain self-association. This

Table 1
Barrier properties of polyamide 1010 (PA1010) films in terms of water vapor permeability (WVP), limonene permeability (LP), and oxygen permeability (OP) measured at 25 °C and 53% relative humidity (RH).

Polymer film	WVP x 10^{15} (Kg·m/m^2·Pa·s)	LP x 10^{15} (Kg·m/m^2·Pa·s)	OP x 10^{19} (m^3·m/m^2·Pa·s)
PA1010	1.56 ± 0.16 (53% RH)	1.78 ± 0.19 (53% RH)	6.59 ± 0.28 (53% RH)
PA6*	20.60 (90% RH)	-	0.52 (0% RH) / 2.25 (75% RH)
PA12**	3.45 (85% RH)	-	20.50 (0% RH) / 20.21 (50% RH) / 21.64 (85% RH)
PHBV***	1.82 (0% RH)	10.26 (40% RH)	2.10 (60% RH)
PLA***	12.31 (0% RH)	3.30 (40% RH)	22.2 (60% RH)
PBAT***	33.13 ± 1.46 (0% RH)	72.58 ± 3.07 (40% RH)	91.4 ± 8.6 (60% RH)

Literature data for polyamide 6 (PA6), polyamide 66 (PA66), polyamide 12 (PA12), poly(3-hydroxybutyrate-*co*-3-hydroxyvalerate) (PHBV), polylactide (PLA), and poly(butylene adipate-*co*-terephthalate) (PBAT): * (Lagarón, 2011), * * (McKeen, 2017), and * ** (Quiles-Carrillo et al., 2019).

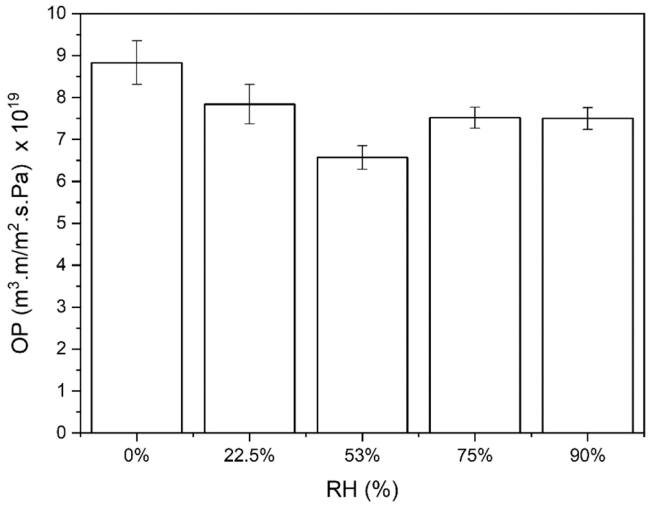

Fig. 7. Evolution of oxygen permeability (OP) as a function of the percentage of relative humidity (% RH) of polyamide 1010 (PA1010) film.

phenomenon has been deeply studied for high-oxygen-barrier poly (ethylene-*co*-vinyl alcohol) (EVOH) due to its technical issue related to "retort shock" (Melendez-Rodriguez et al., 2021). Briefly, at low moisture environments, this level of sorbed water is not high enough to create strong interchain hydrogen bonds, which increases free volume and creates passages for diffusion of oxygen molecules. As opposite, at high %RH, permeability increases due to a phenomenon of water-induced plasticization. In comparison to PA6, with values ranging from 0.52×10^{-19} $m^3 \cdot m/m^2 \cdot Pa \cdot s$ (0% RH) to 2.25×10^{-19} $m^3 \cdot m/m^2 \cdot Pa \cdot s$ (75% RH) (McKeen, 2017), the effect of water on the oxygen permeability variation is considerably lower, which opens up the use of PA1010 as monomaterial packaging. Although the effect of humidity on PA12 is lower, with values within the $2.0–2.2 \times 10^{-18}$ $m^3 \cdot m/m^2 \cdot Pa \cdot s$ range for RH from 0% to 85% (McKeen, 2017), the barrier performance is still one order of magnitude lower. Thus, the use of PA1010 combines the benefit of medium barrier to oxygen with low effect of %RH.

3.6. Shelf-life evaluation of pork meat packaged in PA1010 films

To ascertain the potential of PA1010 in food packaging, the film samples were used as thermosealed bags to package fresh pork fillets and their quality was analyzed for up to 15 days. Fig. 8 provides the visual aspect of the fillets of pork meat packaged in the PA1010 films at different times when stored in refrigeration conditions, that is, at 5 °C with a RH of 48%. One can easily notice that the meat fillets developed reddish and yellowish tonalities after one week of storage, that is, in the samples packaged in PA1010 films for 11 and 15 days.

Table 2 shows, as a function of the storage time, the evolution of pH, weight loss, and optical properties of the packaged meat in the PA1010 films. The fresh pork fillets showed an initial pH of nearly 5.5, which habitually ranges from 5.10 to 6.36 (Xiong et al., 2020). One can observe that the packaged meat developed slightly higher values, being

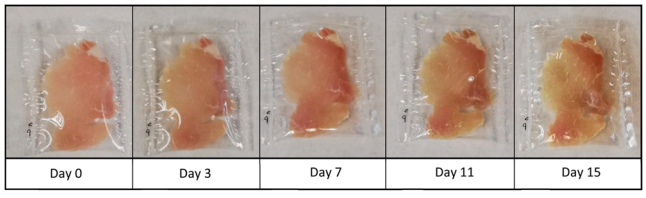

Fig. 8. Images of the pork meat fillets packaged in the polyamide 1010 (PA1010) films during storage.

Table 2
Changes in weight loss (%), pH, and optical properties of the pork meat samples packaged in the polyamide 1010 (PA1010) films during storage.

	Storage time (days)				
	0	3	7	11	15
Weight loss (%)	-	0.211 ± 0.012^{d}	0.400 ± 0.080^{c}	0.754 ± 0.040^{b}	0.971 ± 0.090^{a}
pH	5.49 ± 0.01^{c}	5.44 ± 0.01^{c}	5.40 ± 0.04^{c}	5.66 ± 0.04^{b}	6.07 ± 0.02^{a}
L*	66.7 ± 2.0^{bc}	64.2 ± 0.6^{c}	65.2 ± 2.0^{bc}	68.1 ± 1.0^{ab}	67.3 ± 2.0^{ab}
C_{ab}*	17.6 ± 0.2^{b}	13.7 ± 1.0^{c}	19.5 ± 2.2^{ab}	20.3 ± 1.3^{a}	20.8 ± 2.1^{a}
h_{ab}*	67.0 ± 0.5^{c}	72.0 ± 0.8^{b}	74.0 ± 1.3^{ab}	73.0 ± 1.2^{b}	75.0 ± 0.6^{a}
ΔE_{ab}*	-	3.7 ± 0.6^{b}	4.1 ± 0.6^{b}	6.0 ± 0.9^{a}	7.1 ± 1.3^{a}

Lightness (L*); Chroma (C_{ab}*); Hue (h_{ab}*); total color difference (ΔE_{ab}*).
$^{a-d}$ Different superscripts within the same row indicate significant differences due to storage time for the same sample ($p < 0.05$).

significantly different ($p < 0.05$) only after one week of the storage (day 11). However, these were always within the range favored by consumers, that is, 5.7–6.1 (Kim et al., 2016). In this regard, it has been recently observed that the pH of unpackaged fillets of pork meat that were simply wrapped in polyvinyl chloride (PVC) cling films, increased to values above 7 after one week of storage under the same refrigeration conditions (Hernández-García et al., 2022c). This pH increase is related to the higher content of nitrogenous bases that are produced by proteolysis due to the activity of microorganisms (Daniloski et al., 2019). For example, the use of bioplastic films made of chitosan has recently showed a similar pH increase in fresh poultry meat, from 6.3 (initial day) up to 6.9 (day 15) (Pires et al., 2022).

Moreover, in terms of weight loss, it can be observed that the packaged pork meat in PA1010 showed a significant ($p < 0.05$) but relatively low increase with the storage time, reaching a value close to 1%. This loss of mass can be ascribed to the evaporation of water from the exudate, being originated from the cut surface due to the leakage of intramuscular fluids (Stella et al., 2019). This value is in the range of that observed for pork meat fillets packaged in 100-μm high-barrier multilayer films, based on EVOH, and considerably lower than that in 20-μm PLA films (Hernández-García et al., 2022c). In particular, the latter biopolymer films yielded a weight loss value over 14%. Therefore, the low value attained herein confirms the high barrier performance in terms of water vapor of the tested PA1010 monolayer films and their good potential to protect food products from moisture.

In relation to the optical properties, results revealed that the packaged pork meat fillets developed a significant ($p < 0.05$) color change from day 11 of storage. Discoloration or development of a yellow color in meat is frequently linked to oxidation of both lipids and myoglobin (Mb) (Faustman et al., 2010; Kim et al., 2010). In particular, meat yellowness can be developed due to increases in the oxymyoglobin and metmyoglobin (MbO_2 and MetMb) levels, which are the oxygenated and oxidized forms of Mb (Karamucki et al., 2013). This result suggests that the medium-oxygen-barrier performance of PA1010 can successfully protect meat products for up to one week in refrigeration conditions. However, materials with higher oxygen barrier would be needed for extended periods.

Furthermore, lipid oxidation in the packaged meat was further analyzed by monitoring TBARS formation prior and after the storage period, which measures the MDA amount produced from polyunsaturated fatty acid peroxidation of secondary products (Song et al., 2014). The TBARS value of fresh meat sample was 0.31 ± 0.05 mg MDA/kg meat sample and, when packaged in the PA1010 films, it reached a value of 0.93 ± 0.04 mg MDA/kg at the end of the storage. This is approximately two times lower than the value attained in our previous study for unpackaged pork meat, which yielded a TBARS of

1.90 mg MDA/kg after 15 days of storage at 5 °C (Hernández-García et al., 2022c). Moreover, the oxidation level of the same pork meat when packaged in different high-barrier multilayer and PLA biopolymer films resulted in values in the 0.4–0.8 MDA/kg range and 1.19 MDA/kg, respectively (Hernández-García et al., 2022c). In relation to the performance of other biopolymers, it was reported that fresh poultry meat packaged in chitosan/montmorillonite (MMT) films reached a value of 1.11 MDA/kg when it was also stored under refrigeration for 15 days (Souza et al., 2018). In any case, as similar to in the case of the other film samples, the meat packaged in PA1010 exceeded after 2 weeks of storage the threshold of off-odor perception by consumers, which corresponds to a TBARS value of 0.5 mg MDA/kg sample (Remya et al., 2016). Therefore, the results of lipid oxidation are in agreement with the intermediate barrier performance to oxygen of PA1010 reported above, confirming the need to develop novel technical solutions to extend the meat shelf life for periods longer than 7 days.

Finally, the microbial study of the packaged pork meat was performed since this is a main factor determining its shelf life. Fig. 9 provides the changes in the bacterial counts of LAB, TAC, and coliform counts as a function of the storage time. In terms of LAB, which represent for meat and vacuum-packaged meat products the dominant group (Qin et al., 2013), it was observed that in the meat packaged bacterial counts increased after 1 week of storage from 1.3 log CFU/g to approximately 5 log CFU/g. Then, during the whole storage period, these remained almost constant. In the case of the microbial counts of the total coliforms, it also increased from nearly 1.5 log CFU/g, during the first week, to a value of approximately of 2.5 log CFU/g and then to 5 log CFU/g during the second week of storage. The resultant profile of bacterial growth attained in these packaged meat fillets was in the range to that reported for high-barrier multilayers, which were shown to effectively preserve during storage at 5 °C the microbiological quality of meat pork (Hernández-García et al., 2022c). For TAC, which represents important microbiological indicator since it is used as the quantitative standard for identifying the degree of contamination in meat (Huang et al., 2013), it can be observed that counts for the pork meat packaged in the PA1010 films were kept at 2–3 log CFU/g during the first days of storage. However, at the end of storage, it increased progressively up to nearly 7 log CFU/g. Since, in mechanically separated fresh pork meat, the maximum acceptable level for TAC is 5 log CFU/g according to the microbiological criteria of the European Commission (EC) Regulation Number 2073/2005 on foodstuffs (European Commission, 2005), the microbial analysis performed herein indicates that pork meat can be safely stored at 5 °C in PA1010 films for up one week, whereas the refrigerated storage should not exceed 11 days.

Therefore, the results of the microbial analysis of pork meat fully correlates to the above-reported trend in barrier properties and pH. These indicate that PA1010 films can accomplish the requested values of quality and safety for up to seven days of storage in refrigeration conditions.

4. Conclusions

Current scenarios in sustainable food packaging require the use of high-performance biopolymers to reduce food waste. However, the packaging industry of fresh foodstuffs is still based on multilayer plastic materials derived from non-renewable resources that are technically unfeasible or very difficult to recycle. At the same time, novel biodegradable polyesters currently do not offer the processability and/or properties demanded to achieve packaging materials with the necessary food quality and safety requirements. In this scenario, the present study reports on the synthesis of PA1010, a fully bio-based polyamide, by polycondensation using a “nylon salt” prepared with castor oil derived decamethylenediamine and sebacic acid monomers. The newly produced biopolymer was thereafter shaped into films by cast extrusion, leading to highly transparent films with high thermal, mechanical, and barrier properties to water and limonene vapors and oxygen gas. Finally,

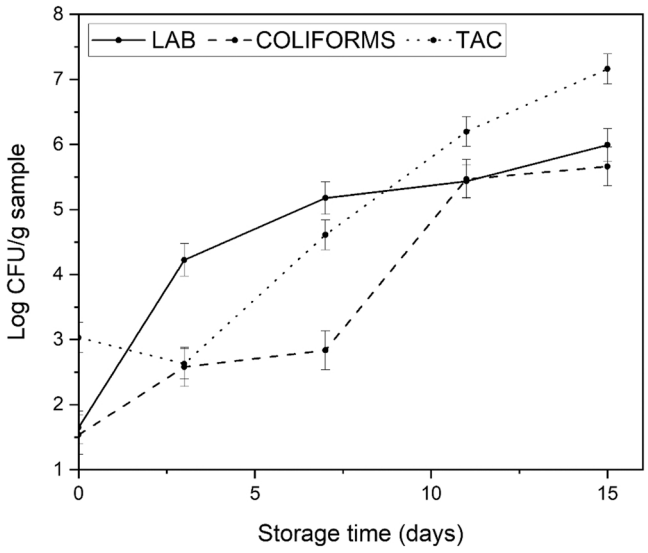

Fig. 9. Changes in microbial counts, expressed as $\log_{10}$ colony-forming units per gram (log CFU/g), in pork meat samples packaged in the PA1010 films during storage: lactic acid bacteria (LAB), coliforms, and total aerobic counts (TAC).

the PA1010 films were used in the form of thermosealed bags to preserve the physicochemical and microbiological properties of fresh pork fillets. The newly developed fully bio-based polyamide films successfully preserved the meat samples for one week at refrigeration conditions. Although the PA1010 films are still outperformed by high-barrier multilayer structures, these can still represent a sustainable alternative to package food products requiring moderate barrier or lower shelf life. Therefore, PA1010 can be applied for the design of monolayer packaging articles for applications of food preservation, such as trays and lids, that are fully based on renewable material and easily recycled after use. In any case, future studies should analyze the actual secondary (melt reprocessing) and tertiary (chemical depolymerization and repolymerization) recycling technology of the PA1010 monolayer films to confirm the sustainable loop model proposed herein.

CRediT authorship contribution statement

E. Hernández-García: Methodology, Validation, Formal analysis, Writing – original draft. **M. Pacheco-Romeralo**: Methodology, Validation, Formal analysis. **L. Pascual-Ramírez**: Methodology, Validation, Formal analysis. **M. Vargas**: Conceptualization, Validation, Writing – review & editing. **S. Torres-Giner**: Conceptualization, Methodology, Validation, Formal analysis, Writing – review & editing, Supervision, Project administration, Funding acquisition. All authors have read and agreed to the published version of the manuscript.

Data availability

Data will be made available on request.

Acknowledgments

This work was carried out with the financial support of the Ramón y Cajal contract (RYC2019–027784-I) from the Spanish Ministry of Science and Innovation (MICI) and the program “Garantía Juvenil” (EDGJID/2021/290) from Generalitat Valenciana (GVA).

References

Ahmad, A. A., & Sarbon, N. M. (2021). A comparative study: Physical, mechanical and antibacterial properties of bio-composite gelatin films as influenced by chitosan and

zinc oxide nanoparticles incorporation. *Food Bioscience, 43*. https://doi.org/10.1016/j.fbio.2021.101250
Alias, A. R., Wan, M. K., & Sarbon, N. M. (2022). Emerging materials and technologies of multi-layer film for food packaging application: A review. *Food Control, 136*, Article 108875. https://doi.org/10.1016/j.foodcont.2022.108875
Amit, S. K., Uddin, M. M., Rahman, R., Rezwanul Islam, S. M., & Samad Khan, M. (2017). A review on mechanisms and commercial aspects of food preservation and processing. *Agriculture & Food Security, 6*, 51. https://doi.org/10.1186/s40066-017-0130-8
Arrieta, M. P., Samper, M. D., López, J., & Jiménez, A. (2014). Combined effect of poly (hydroxybutyrate) and plasticizers on polylactic acid properties for film intended for food packaging. *Journal of Polymers and the Environment, 22*, 460–470. https://doi.org/10.1007/s10924-014-0654-y
ASTM D882; Standard Test Method for Tensile Properties of Thin Plastic Sheeting. Annual Book of ASTM Standards. American Society for Testing and Materials: Philadelphia, PA, USA, 2001; pp. 162–170.
ASTM E96–95; Standard Test Methods for Water Vapor Transmission of Materials. ASTM, Annual Book of ASTM Standards. American Society for Testing and Materials: Philadelphia, PA, USA, 1995; pp. 406–413.
ASTM D3985–05; Standard Test Method for Oxygen Gas Transmission Rate through Plastic Film and Sheeting using a Coulometric Sensor. Annual Book of ASTM Standards. American Society for Testing and Materials: Philadelphia, PA, USA, 2010; pp. 1–7.
Češarek, U., Pahovnik, D., & Žagar, E. (2020). Chemical recycling of aliphatic polyamides by microwave-assisted hydrolysis for efficient monomer recovery. *ACS Sustainable Chemistry & Engineering, 8*, 16274–16282. https://doi.org/10.1021/acssuschemeng.0c05706
Chen, G., Tang, K., Niu, G., Pan, K., Feng, X., & Zhang, L. (2019). Synthesis and characterization of the novel nylon 12 6 based on 1,12-diaminododecane. *Polymer Engineering & Science, 59*, 192–197. https://doi.org/10.1002/pen.24888
Cho, J. W., & Paul, D. R. (2001). Nylon 6 nanocomposites by melt compounding. *Polymer, 42*, 1083–1094. https://doi.org/10.1016/S0032-3861(00)00380-3
Cozzolino, C. A., Cerri, G., Brundu, A., & Farris, S. (2014). Microfibrillated cellulose (MFC): Pullulan bionanocomposite films. *Cellulose, 21*, 4323–4335. https://doi.org/10.1007/s10570-014-0433-x
Cui, X., Liu, Z., & Yan, D. (2004). Synthesis and characterization of novel even–odd nylons based on undecanedioic acid. *European Polymer Journal, 40*, 1111–1118. https://doi.org/10.1016/j.eurpolymj.2003.12.021
Cui, X., & Yan, D. (2005). Preparation, characterization and crystalline transitions of odd–even polyamides 11,12 and 11,10. *European Polymer Journal, 41*, 863–870. https://doi.org/10.1016/j.eurpolymj.2004.10.045
Daniloski, D., Petkoska, A. T., Galić, K., Ščetar, M., Kurek, M., Vaskoska, R., Kalevska, T., & Nedelkoska, D. N. (2019). The effect of barrier properties of polymeric films on the shelf-life of vacuum packaged fresh pork meat. *Meat Science, 158*, Article 107880. https://doi.org/10.1016/j.meatsci.2019.107880
Del Nobile, M. A., Buonocore, G. G., Palmieri, L., Aldi, A., & Acierno, D. (2002). Moisture transport properties of polyamides copolymers intended for food packaging applications. *Journal of Food Engineering, 53*, 287–293. https://doi.org/10.1016/S0260-8774(01)00167-4
European Commission, 2005. Commission Regulation (EC) No 2073/2005 of 15 November 2005 on microbiological criteria for foodstuffs. Commission Regulation (EC) No 2073/2005 of 15 November 2005 on Microbiological Criteria for Foodstuffs. ⟨http://data.europa.eu/eli/reg/2005/2073/oj⟩.
Faustman, C., Sun, Q., Mancini, R., & Suman, S. P. (2010). Myoglobin and lipid oxidation interactions: Mechanistic bases and control. *Meat Science, 86*, 86–94. https://doi.org/10.1016/j.meatsci.2010.04.025
Gupta, V. B., & Rana, S. K. (1998). Double yield in tensile deformation of high-density polyethylene fiber. *Journal of Macromolecular Science, Part B, 37*, 783–804. https://doi.org/10.1080/00222349808212417
Hernández-García, E., Vargas, M., González-Martínez, C., & Chiralt, A. (2021). Biodegradable antimicrobial films for food packaging: effect of antimicrobials on degradation. *Foods, 10*, 1256. https://doi.org/10.3390/foods10061256
Hernández-García, E., Vargas, M., & Chiralt, A. (2022a). Active starch-polyester bilayer films with surface-incorporated ferulic acid. *Membranes, 12*, 976. https://doi.org/10.3390/membranes12100976
Hernández-García, E., Vargas, M., & Chiralt, A. (2022b). Starch-polyester bilayer films with phenolic acids for pork meat preservation. *Food Chemistry, 385*, Article 132650. https://doi.org/10.1016/j.foodchem.2022.132650
Hernández-García, E., Vargas, M., & Torres-Giner, S. (2022c). Quality and shelf-life stability of pork meat fillets packaged in multilayer polylactide films. *Foods, 11*(3), 426. https://doi.org/10.3390/foods11030426
Hernández-García, E., Chiralt, A., Vargas, M., & Torres-Giner, S. (2023). Lid Films of Poly (3-hydroxybutyrate-*co*-3-hydroxyvalerate)/microfibrillated cellulose composites for fatty food preservation. *Foods, 12*, 375. https://doi.org/10.3390/foods12020375
Huang, L., Zhao, J., Chen, Q., & Zhang, Y. (2013). Rapid detection of total viable count (TVC) in pork meat by hyperspectral imaging. *Food Research International, 54*, 821–828. https://doi.org/10.1016/j.foodres.2013.08.011
Hutchings, J.B. 1999. Instrumental specification. In Food colour and appearance (pp. 199–237). https://doi.org/10.1007/978–1-4615–2373-4_7.
Kaiser, K., Schmid, M., Schlummer, M., 2018. Recycling of Polymer-Based Multi-layer Packaging: A Review. Recycling 3, 1. ⟨https://doi.org/10.3390/recycling3010001⟩.
Karamucki, T., Jakubowska, M., Rybarczyk, A., & Gardzielewska, J. (2013). The influence of myoglobin on the colour of minced pork loin. *Meat Science, 94*, 234–238. https://doi.org/10.1016/j.meatsci.2013.01.014
Kim, G. D., Jeong, J. Y., Hur, S. J., Yang, H. S., Jeon, J. T., & Joo, S. T. (2010). The relationship between meat color (CIE L* and a *), myoglobin content, and their influence on muscle fiber characteristics and pork quality. *Korean Journal for Food Science of Animal Resources, 30*, 626–633. https://doi.org/10.5851/kosfa.2010.30.4.626
Kim, T. W., Kim, C. W., Kwon, S. G., Hwang, J. H., Park, D. H., Kang, D. G., Ha, J., Yang, M. R., Kim, S. W., & Kim, I. S. (2016). pH as analytical indicator for managing pork meat quality. *Sains Malaysiana, 45*, 1097–1103.
Lagarón, J. M. (2011). 1 - Multifunctional and nanoreinforced polymers for food packaging. In J.-M. Lagarón (Ed.), *Multifunctional and Nanoreinforced Polymers for Food Packaging* (pp. 1–28). Woodhead Publishing. https://doi.org/10.1533/9780857092786.1.
Li, Y., Zhang, G., & Yan, D. (2003). Synthesis and crystallization behavior of nylon 12,14. I. Preparation and melting behavior. *Journal of Applied Polymer Science, 88*, 1581–1589. https://doi.org/10.1002/app.11826
Logakis, E., Pandis, C., Peoglos, V., Pissis, P., Stergiou, C., Pionteck, J., Pötschke, P., Mičušík, M., & Omastová, M. (2009). Structure–property relationships in polyamide 6/multi-walled carbon nanotubes nanocomposites. *Journal of Polymer Science Part B: Polymer Physics, 47*, 764–774. https://doi.org/10.1002/polb.21681
McKeen, L. W. (2017). 8 - Polyamides (Nylons). In L. W. McKeen (Ed.), *Film Properties of Plastics and Elastomers* (Fourth edition.,, pp. 187–227). William Andrew Publishing.
Melendez-Rodriguez, B., Torres-Giner, S., Zavagna, L., Sammon, C., Cabedo, L., Prieto, C., & Lagaron, J. M. (2021). Development and Characterization of Electrospun Fiber-Based Poly(ethylene-*co*-vinyl Alcohol) Films of Application Interest as High-Gas-Barrier Interlayers in Food Packaging. *Polymers, 13*, 2061. https://doi.org/10.3390/polym13132061
Mousavi Khaneghah, A., Hashemi, S. M. B., & Limbo, S. (2018). Antimicrobial agents and packaging systems in antimicrobial active food packaging: An overview of approaches and interactions. *Food and Bioproducts Processing, 111*, 1–19. https://doi.org/10.1016/j.fbp.2018.05.001
Pardo, G., & Zufía, J. (2012). Life cycle assessment of food-preservation technologies. *Journal of Cleaner Production, 28*, 198–207. https://doi.org/10.1016/j.jclepro.2011.10.016
Philp, C., Ritchie, R. J., & Guy, K. (2013). Biobased plastics in a bioeconomy. *Trends in Biotechnology, 31*(2), 65–67. https://doi.org/10.1016/j.tibtech.2012.11.009
Pires, J. R. A., Almeida, K. M., Augusto, A. S., Vieira, É. T., Fernando, A. L., & Souza, V. G. L. (2022). Application of Biocomposite Films of Chitosan/Natural Active Compounds for Shelf Life Extension of Fresh Poultry Meat. *Journal of Composites Science, 6*, 342. https://doi.org/10.3390/jcs6110342
Qin, Y.-Y., Yang, J.-Y., Lu, H.-B., Wang, S.-S., Yang, J., Yang, X.-C., Chai, M., Li, L., & Cao, J.-X. (2013). Effect of chitosan film incorporated with tea polyphenol on quality and shelf life of pork meat patties. *International Journal of Biological Macromolecules, 61*, 312–316. https://doi.org/10.1016/j.ijbiomac.2013.07.018
Quiles-Carrillo, L., Montanes, N., Boronat, T., Balart, R., & Torres-Giner, S. (2017). Evaluation of the engineering performance of different bio-based aliphatic homopolyamide tubes prepared by profile extrusion. *Polymer Testing, 61*, 421–429. https://doi.org/10.1016/j.polymertesting.2017.06.004
Quiles-Carrillo, L., Montanes, N., Pineiro, F., Jorda-Vilaplana, A., & Torres-Giner, S. (2018). Ductility and Toughness Improvement of Injection-Molded Compostable Pieces of Polylactide by Melt Blending with Poly(ε-caprolactone) and Thermoplastic Starch. *Materials, 11*, 2138. https://doi.org/10.3390/ma11112138
Quiles-Carrillo, L., Montanes, N., Lagaron, J. M., Balart, R., & Torres-Giner, S. (2019). In Situ Compatibilization of Biopolymer Ternary Blends by Reactive Extrusion with Low-Functionality Epoxy-Based Styrene–Acrylic Oligomer. *Journal of Polymers and the Environment, 27*, 84–96. https://doi.org/10.1007/s10924-018-1324-2
Quiles-Carrillo, L., Montanes, N., Fombuena, V., Balart, R., & Torres-Giner, S. (2020). Enhancement of the processing window and performance of polyamide 1010/bio-based high-density polyethylene blends by melt mixing with natural additives. *Polymer International, 69*, 61–71. https://doi.org/10.1002/pi.5919
Remya, S., Mohan, C. O., Bindu, J., Sivaraman, G. K., Venkateshwarlu, G., & Ravishankar, C. N. (2016). Effect of chitosan based active packaging film on the keeping quality of chilled stored barracuda fish. *Journal of Food Science and Technology, 53*, 685–693. https://doi.org/10.1007/s13197-015-2018-6
Rhee, S., & White, J. L. (2002). Crystal structure, morphology, orientation, and mechanical properties of biaxially oriented polyamide 6 films. *Polymer, 43*, 5903–5914. https://doi.org/10.1016/S0032-3861(02)00489-5
Roohi, Srivastava, Bano, P., Zaheer, K., & Kuddus, M, M. R. (2018). Biodegradable Smart Biopolymers for Food Packaging: Sustainable Approach Toward Green Environment. In S. Ahmed (Ed.), *Bio-based Materials for Food Packaging: Green and Sustainable Advanced Packaging Materials* (pp. 197–216). Singapore, Singapore: Springer. https://doi.org/10.1007/978-981-13-1909-9_9.
Rosenboom, J. G., Langer, R., & Traverso, G. (2022). Bioplastics for a circular economy. *Nature Reviews Materials, 7*, 117–137. https://doi.org/10.1038/s41578-021-00407-8
Shan, G.-F., Yang, W., Xie, B.-h, Li, Z.-m, Chen, J., & Yang, M.-b (2005). Double yielding behaviors of polyamide 6 and glass bead filled polyamide 6 composites. *Polymer Testing, 24*, 704–711. https://doi.org/10.1016/j.polymertesting.2005.05.003
Shan, G.-F., Yang, W., Yang, M.-b, Xie, B.-h, Feng, J.-m, & Fu, Q. (2007). Effect of temperature and strain rate on the tensile deformation of polyamide 6. *Polymer, 48*, 2958–2968. https://doi.org/10.1016/j.polymer.2007.03.013
Siu, G. M., & Draper, H. H. (1978). A survey of the malonaldehyde content of retail meats and fish. *Journal of Food Science, 43*, 1147–1149. https://doi.org/10.1111/j.1365-2621.1978.tb15256.x
Song, N.-B., Lee, J.-H., Al Mijan, M., & Song, K. B. (2014). Development of a chicken feather protein film containing clove oil and its application in smoked salmon packaging. *LWT - Food Science and Technology, 57*, 453–460. https://doi.org/10.1016/j.lwt.2014.02.009
Souza, V. G. L., Pires, J. R. A., Vieira, É. T., Coelhoso, I. M., Duarte, M. P., & Fernando, A. L. (2018). Shelf Life Assessment of Fresh Poultry Meat Packaged in

Novel Bionanocomposite of Chitosan/Montmorillonite Incorporated with Ginger Essential Oil. *Coatings, 8*, 177. https://doi.org/10.3390/coatings8050177

Stella, S., Garavaglia, D., Francini, G., Viganò, V., Bernardi, C., & Tirloni, E. (2019). Evaluation of the weight loss of raw beef cuts vacuumpackaged with two different techniques. *Italian Journal of Food Safety, 8*. https://doi.org/10.4081/ijfs.2019.8111

Sun, L., Li, H.-b, Huang, Y.-q, Wu, J.-w, Runt, J., Kuo, M.-c, Huang, K.-s, & Yeh, J.-t (2019). Oxygen barrier, free volume and miscibility properties of fully bio-based polyamide 1010/poly(vinyl alcohol) blends. *Journal of Polymer Research, 26*, 166. https://doi.org/10.1002/app.48562

Torres-Giner, S., Figueroa-Lopez, K. J., Melendez-Rodriguez, B., Prieto, C., Pardo-Figuerez, M., & Lagaron, J. M. (2021). Emerging Trends in Biopolymers for Food Packaging. *Sustainable Food Packaging Technology*, 1–33. https://doi.org/10.1002/9783527820078.ch1

Torres-Giner, S., Gil, L., Pascual-Ramírez, L., & Garde-Belza, J., A. (2019). Packaging: Food Waste Reduction. *Encyclopedia of Polymer Applications*. CRC Press,.

UNE-EN ISO 307:2007. 2007. Asociación Española de Normalización. Plásticos. Poliamidas. Determinación del índice de viscosidad (ISO 307:2007). Asociación Española de Normalización: Madrid, Spain, 2007.

Winnacker, M., & Rieger, B. (2016). Biobased Polyamides: Recent Advances in Basic and Applied Research. *Macromolecular Rapid Communications, 37*, 1391–1413. https://doi.org/10.1002/marc.201600181

Wohner, B., Pauer, E., Heinrich, V., & Tacker, M. (2019). Packaging-Related Food Losses and Waste: An Overview of Drivers and Issues. *Sustainability, 11*, 264. https://doi.org/10.3390/su11010264

Wudy, K., & Drummer, D. (2019). Aging effects of polyamide 12 in selective laser sintering: Molecular weight distribution and thermal properties. *Additive Manufacturing, 25*, 1–9. https://doi.org/10.1016/j.addma.2018.11.007

Xiong, Y., Chen, M., Warner, R. D., & Fang, Z. (2020). Incorporating nisin and grape seed extract in chitosan-gelatine edible coating and its effect on cold storage of fresh pork. *Food Control, 110*, Article 107018. https://doi.org/10.1016/j.foodcont.2019.107018

Yan, C., Hao, L., Xu, L., & Shi, Y. (2011). Preparation, characterisation and processing of carbon fibre/polyamide-12 composites for selective laser sintering. *Composites Science and Technology, 71*, 1834–1841. https://doi.org/10.1016/j.compscitech.2011.08.013

Yan, M., & Yang, H. (2012). Improvement of polyamide 1010 with silica nanospheres via in situ melt polycondensation. *Polymer Composites, 33*, 1770–1776. https://doi.org/10.1002/pc.22318